

# Perinatal and Postnatal Expression of Cav1.3 $\alpha_{1D}$ $Ca^{2+}$ Channel in the Rat Heart

YONGXIA QU, EDDY KARNABI, OMAR RAMADAN, YUANKUN YUE, MOHAMED CHAHINE, AND MOHAMED BOUTJDIR

*Molecular and Cellular Cardiology Program [Y.Q., E.K., O.R., Y.Y., M.B.], VA New York Harbor Healthcare System, Brooklyn, NY, 11209; Department of Medicine [Y.Q., M.B.], SUNY Downstate Medical Center, Brooklyn, NY 11203; Department of Medicine [E.K.], Hospital of St. Raphael, New Haven, CT 06511; Department of Medicine [M.C.], Le Centre de Recherche Université Laval Robert-Giffard, Laval University, Quebec G1J 2G3, Canada*

**ABSTRACT:** The novel Cav1.3 ( $\alpha_{1D}$ ) L-type  $Ca^{2+}$  channel plays a significant role in sinoatrial (SA) and atrioventricular (AV) nodes function and in atrial fibrillation. However, the characterization of  $\alpha_{1D}$   $Ca^{2+}$  channel during heart development is very limited. We used real-time RT-PCR, Western blotting, and indirect immunostaining to characterize the developmental expression and localization of  $\alpha_{1D}$   $Ca^{2+}$  channel in rat hearts. Both protein and mRNA levels of  $\alpha_{1D}$   $Ca^{2+}$  channel decreased postnatally. Two forms of  $\alpha_{1D}$   $Ca^{2+}$  channel protein (250 and 190 kD) were observed, with the full-length (250 kD) channel protein being predominant in the prenatal stages. Both Western blots and confocal imaging demonstrated that  $\alpha_{1D}$   $Ca^{2+}$  channel protein was expressed in both atria and ventricles at fetal and neonatal stages but was absent in the adult ventricles. Interestingly,  $\alpha_{1D}$   $Ca^{2+}$  channel was also found at the nucleus/perinucleus of immature but not adult atrial cells. Furthermore, the nuclear staining was reproduced in adult atrial cell line, HL-1 cells, which possess immature properties. The data are first to show that  $\alpha_{1D}$   $Ca^{2+}$  channel has unique age-dependent expression profile and subcellular localization in the heart, suggesting a developmental stage-dependent specific function. (*Pediatr Res* 69: 479–484, 2011)

The L-type  $Ca^{2+}$  channel is a heterologomeric complex of  $\alpha_1$ ,  $\beta$ , and  $\alpha_2/\delta$  subunits (1). Four genes encode L-type  $Ca^{2+}$  channel  $\alpha_1$  subunits in mammals ( $\alpha_{1C}$ ,  $\alpha_{1S}$ ,  $\alpha_{1D}$ , and  $\alpha_{1F}$ ) (1,2).  $\alpha_{1C}$  (Cav1.2) represents the most abundant isoform in the cardiovascular system, whereas  $\alpha_{1D}$  (Cav1.3) is expressed in neurons and neuroendocrine cells (3,4). It is therefore believed that the contribution of L-type  $Ca^{2+}$  current ( $I_{Ca-L}$ ) to the physiology/pathophysiology of the heart is mainly mediated through  $\alpha_{1C}$   $Ca^{2+}$  channel.

The functional role of  $\alpha_{1D}$  in the heart has been addressed by several published reports (5–7), including from our laboratory (8). The emerging consensus is that because of the low activation voltage (–60 to –50 mV) and abundant expression in the sinoatrial (SA) and atrioventricular (AV) nodes,  $\alpha_{1D}$  plays an important role in the pacemaker activity and action potential conduction at the AV node. This is further supported by data showing that genetic deletion of  $\alpha_{1D}$  causes sinus bradycardia and various degrees of AV block (5–7) and makes

this mouse prone to atrial fibrillation (8). Compared with  $\alpha_{1C}$ , the  $\alpha_{1D}$   $Ca^{2+}$  channel has less sensitivity to dihydropyridines (1,9,10). Despite these subtle differences, to date, there are no available pharmacological or biophysical approaches to functionally dissect  $\alpha_{1D}$  from  $\alpha_{1C}$   $Ca^{2+}$  current in the native tissue.

Developmental change of the  $\alpha_{1C}$   $Ca^{2+}$  channel in the heart has been extensively studied (11,12). Lower  $\alpha_{1C}$   $Ca^{2+}$  channel expression levels have been demonstrated in immature hearts, followed by an increase with cardiac maturation in both rat and human (11,13). It is generally believed that a higher expression of the T-type  $Ca^{2+}$  channel and the Na/Ca exchanger compensate for the low levels of the  $\alpha_{1C}$   $Ca^{2+}$  channel and enable the immature heart to maintain functional contractility. However, there is very limited information on the developmental changes of the  $\alpha_{1D}$   $Ca^{2+}$  channel in the heart. This study is the first to characterize the expression levels of the  $\alpha_{1D}$   $Ca^{2+}$  channel and its subcellular localization during development in the rat heart.

## METHODS

**Use of rats.** Fetal (17- to 20-d gestation), neonate (1- to 3-d old), juvenile (4- to 6-wk-old), and adult (6- to 8-mo-old) Sprague-Dawley rats of either sex used in this study were approved by IACUC at VA New York Harbor Healthcare System.

**Real-time RT-PCR.** TaqMan real-time RT-PCR was performed using 18S ribosomal RNA as internal control. Total RNAs were prepared from the atria at various developmental stages as previously described (14,15). Predesigned and labeled primer/Taqman probe sets for  $\alpha_{1D}$  were purchased (Applied Biosystems, CA). The conditions for real-time RT-PCR were preheating at 50°C for 2 min and at 95°C for 10 min, followed by 40 cycles of shuttle heating at 95°C for 15 s and at 60°C for 1 min. The cycle threshold Ct value for each sample that was proportional to the log of the initial amount of input cDNA was calculated and plotted. 18S rRNA was used as internal control.

**Protein extraction and Western blot.** Membrane proteins were prepared as previously described (15). Same amount of membrane proteins (50–100  $\mu$ g) were loaded for each lane of 4–12% SDS polyacrylamide gels. The immunoblots were incubated overnight at 4°C with 1:200 primary anti- $\alpha_{1D}$   $Ca^{2+}$  channel antibodies (Calbiochem, CA), developed with horseradish peroxidase-labeled anti-rabbit antibody, and detected by enhanced chemiluminescence (Amersham, NJ). The density of protein bands was quantified by the National Institutes of Health image software (<http://rsbweb.nih.gov/nih-image/>). Anti- $\alpha_{1D}$  antibody preincubated with its antigenic peptide was included as a negative control.

**Isolation of cardiac myocytes.** Cardiac myocytes of juvenile and adult rats were obtained from Langendorff-perfused hearts as previously described (16). Hearts were perfused at 37°C with a HEPES-buffered solution containing 1.5 mg/mL collagenase type B (Boehringer Mannheim, Germany) for 8–15 min and then dispersed then dispersed in a KB solution containing (mmol/L): K

Received August 26, 2010; accepted December 29, 2010.

Correspondence: Mohamed Boutjdir, Ph.D., Research and Development (151), VA New York Harbor Healthcare System, 800 Poly Place, Brooklyn, NY 11209; e-mail: mohamed.boutjdir@va.gov

Supported by National Institutes of Health [R01 HL-077494], Veterans Affairs MERIT grants [to M.B.], and Veteran Affairs MREP grant [to Y.Q.].

**Abbreviations:**  $I_{Ca-L}$ , L-type  $Ca^{2+}$  current

glutamate 70, KCl 30,  $\text{KH}_2\text{PO}_4$  10,  $\text{MgCl}_2$  1, taurine 20, glucose 10, and HEPES 10. Isolation of fetal and neonatal rat atrial and ventricular myocytes was performed using chopping method with trypsin digestion as described (17), and cells were cultured on cover slips with Dulbecco's Modified Eagle's Medium containing 10% calf serum (GIBCO, CA), 2% penicillin/streptomycin, before use for immunostainings and transfections.

**Maintenance of adult atrial HL-1 cells.** The HL-1 cells were cultured in Claycomb medium supplemented with 10% fetal bovine serum (Invitrogen, CA), 2 mM L-glutamine, 100  $\mu\text{M}$  norepinephrine, 100 U/mL penicillin, and 100  $\mu\text{g}/\text{mL}$  streptomycin on precoated flasks with fibronectin (18).

**Indirect immunofluorescence staining.** Briefly, immunofluorescent stainings were performed as previously described (14). Cardiac cells were permeabilized, blocked, incubated overnight at 4°C with primary anti- $\alpha_{1D}$  antibodies against a peptide [(KY)DNKVTIDDDYQEEADKD] corresponding to residues 809–825 of rat brain  $\alpha_{1D}$  subunit (1:200; Calbiochem, CA, and Sigma Chemical Co., MO), and detected with FITC-conjugated anti-rabbit antibody (1:200; Johnson Immuno, PA) and viewed with a confocal scanning laser microscope (MRC-600; Bio-Rad, CA) using XYZ scan. Surface plot was used to illustrate anti- $\alpha_{1D}$  antibody staining. Secondary antibody alone and anti- $\alpha_{1D}$  antibody preincubated with its antigenic peptide were included as negative controls.

**Statistic analysis.** Statistical comparisons were evaluated using unpaired student *t* test and one-way ANOVA as appropriate. Data are presented as mean  $\pm$  SEM. A value of  $p < 0.05$  is considered significant.

## RESULTS

### Perinatal and postnatal expression level of $\alpha_{1D}$ mRNA.

The  $\alpha_{1D}$   $\text{Ca}^{2+}$  channel mRNA level during heart development was carried out by real-time RT-PCR using total RNA isolated from fetal, neonatal, 4- to 6-wk-old, and 6- to 8-mo-old rat atrial tissue using 18S rRNA as an internal control. For easy comparison, the value of the  $\alpha_{1D}$   $\text{Ca}^{2+}$  channel mRNA at different developmental stages was normalized to that of the fetal stage.  $\alpha_{1D}$   $\text{Ca}^{2+}$  channel mRNA level decreased to 0.70 at neonatal stage, decreased to 0.36 at 4 wk, and reached the lowest level of 0.22 ( $n = 3$ ,  $p < 0.05$ ) at the adult stage. The results from three different experiments are summarized in Figure 1A.

**Perinatal and postnatal expression of  $\alpha_{1D}$   $\text{Ca}^{2+}$  channel protein.** The  $\alpha_{1D}$   $\text{Ca}^{2+}$  channel protein level at various stages was assessed by Western blot and shown in Figure 1B. At the fetal stage (lane 1), a full size (250 kD) and a short form (190 kD) of the  $\alpha_{1D}$   $\text{Ca}^{2+}$  channel protein were observed. At neonatal stage (lane 2), 6-wk-old (lane 3), and 6-mo-old (lane 5) atria, only the short form band was observed. However, none of the  $\alpha_{1D}$   $\text{Ca}^{2+}$  channel protein bands (250 and 190 kD) were observed in the 6-wk (lane 4) and 6-mo ventricles (lane 6). Both the full size and the short form bands were absent when preincubating the anti- $\alpha_{1D}$  antibody with its antigenic peptide (lane 7). The lower panel of Figure 1B shows a band corresponding to nonspecific proteins in each lane demonstrating that the absence of the  $\alpha_{1D}$  protein in the adult stage is not due to a loading error. The  $\alpha_{1D}$   $\text{Ca}^{2+}$  channel protein level decreased postnatally and reached steady level at 6 wk. The value of  $\alpha_{1D}$   $\text{Ca}^{2+}$  channel protein at different developmental stages was normalized to that of the 6-wk and 6-mo-old atria. The  $\alpha_{1D}$   $\text{Ca}^{2+}$  channel protein level was  $12 \pm 2.5$  and  $4.5 \pm 0.6$  fold higher at fetal and neonatal stage, respectively, ( $n = 3$ ,  $p < 0.05$ ).

**Developmental-dependent subcellular localization of the  $\alpha_{1D}$   $\text{Ca}^{2+}$  channel.** Subcellular localization of the  $\alpha_{1D}$   $\text{Ca}^{2+}$  channel was carried out by confocal indirect immunostaining

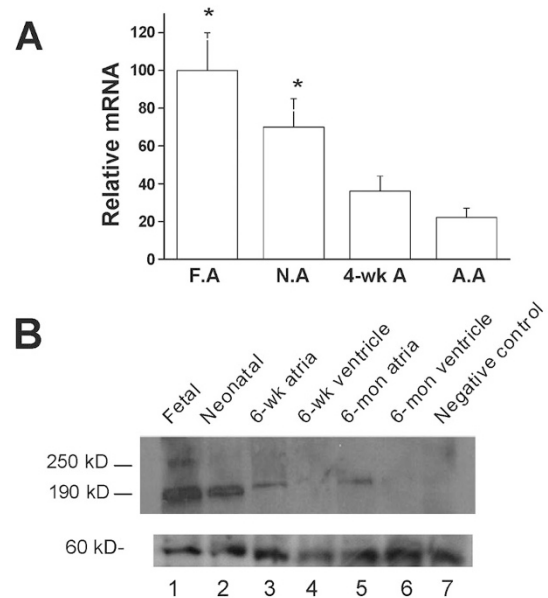


**Figure 1.**  $\alpha_{1D}$   $\text{Ca}^{2+}$  channel mRNA and proteins levels during heart development using real-time PCR and Western blot, respectively. (A)  $\alpha_{1D}$   $\text{Ca}^{2+}$  channel mRNA during rat heart development by real-time RT-PCR using 18S rRNA as internal control. Value of the fetal stage was set at 100 for easy comparison. \* indicates  $p < 0.05$  compared with adult stage. F.A: fetal atria; N.A: neonatal atria; A.A: adult atria. (B) Representative Western blot experiment using anti- $\alpha_{1D}$   $\text{Ca}^{2+}$  channel antibody. Total membrane protein (100  $\mu\text{g}$ ) was loaded in each lane. Lane 1, fetal stage; lane 2, neonatal stage; lane 3, 6-wk atria; lane 4, 6-wk ventricles; lane 5, 6-mo atria; lane 6, 6-mo ventricle; and lane 7, negative control (anti- $\alpha_{1D}$   $\text{Ca}^{2+}$  channel antibody preincubated with antigenic peptide using membrane protein from fetal stage). (B) Lower part: nonspecific protein bands observed in each lane, indicating that absence of  $\alpha_{1D}$  protein in the adult stage is not secondary to loading error.

using the anti- $\alpha_{1D}$  antibody. Sarcolemmal staining was observed in the fetal (Fig. 2A), neonatal (Fig. 2B), 6-wk (Fig. 2C and D), and 6-mo (Fig. 2E) atrial cells. Ventricular cells at both the fetal (Fig. 3A) and neonatal (Fig. 3B) stages showed similar staining pattern to atrial cells (Fig. 2A and B), indicating that the  $\alpha_{1D}$   $\text{Ca}^{2+}$  channel protein is expressed in both the atria and the ventricles of the immature hearts. Interestingly, no staining was observed in the 6-wk and 8-mo-old ventricular cells (Fig. 3C and D). The staining pattern of the  $\alpha_{1D}$   $\text{Ca}^{2+}$  channel in the atrial cells was not observed when using the secondary antibody alone (data not shown) or using the anti- $\alpha_{1D}$  antibody preincubated with its antigenic peptide at the fetal (Fig. 4A), the neonatal (Fig. 4B), 6-wk (Fig. 4C), and 6-mo (Fig. 4D) stages, indicating the specificity of the anti- $\alpha_{1D}$  antibody.

Interestingly, in addition to the sarcolemmal staining, a unique nuclear staining was observed in immature hearts (Figs. 2A and B and 3A and B). This staining pattern was not seen in 6-wk and 6-mo-old rat atrial cells (Fig. 2C–E). The specificity of the nuclear staining was demonstrated by the use of anti- $\alpha_{1D}$  antibodies from two commercial vendors that showed the same staining pattern (data not shown). In addition, the nuclear staining was not observed in the negative control experiments in which the anti- $\alpha_{1D}$  antibody was pre-

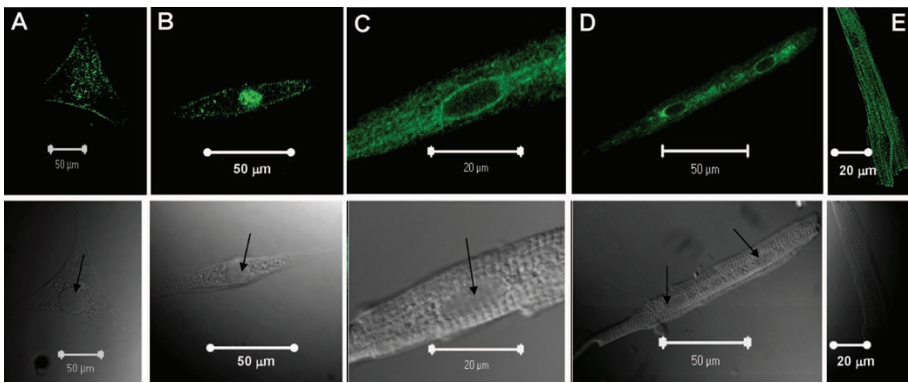


**Figure 2.** Representative confocal images of isolated atrial myocytes using anti- $\alpha_{1D}$   $Ca^{2+}$  channel antibody. The *upper panels* show the staining pattern of the  $\alpha_{1D}$   $Ca^{2+}$  channel protein using FITC-labeled secondary antibody. The *lower panels* show the phase controls of the cells at different developmental stages. *A*, fetal; *B*, neonatal; *C*, 6 wk (amplified from *D*); *D*, 6 wk; *E*, 6 mo. *Arrows* indicate the nucleus.

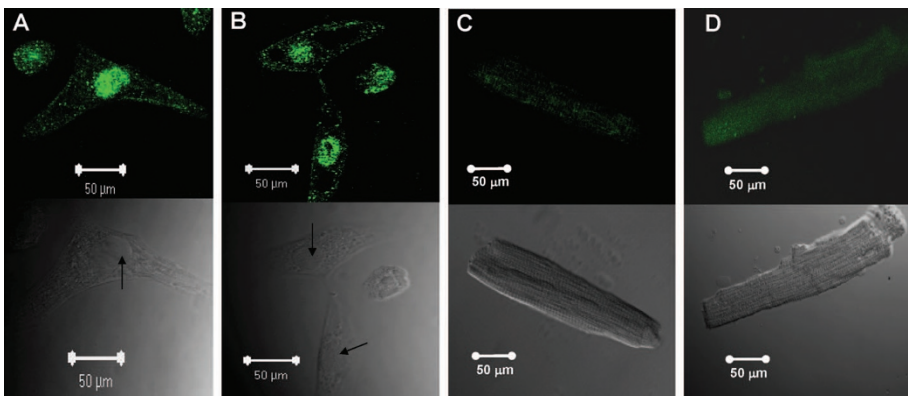


**Figure 3.** Representative confocal images using anti- $\alpha_{1D}$   $Ca^{2+}$  channel antibody on ventricular cells from various developmental stages: *A*, fetal ventricular cells; *B*, neonatal ventricular cells; *C*, 6-wk ventricular cell; *D*, 8-mo ventricular cell.

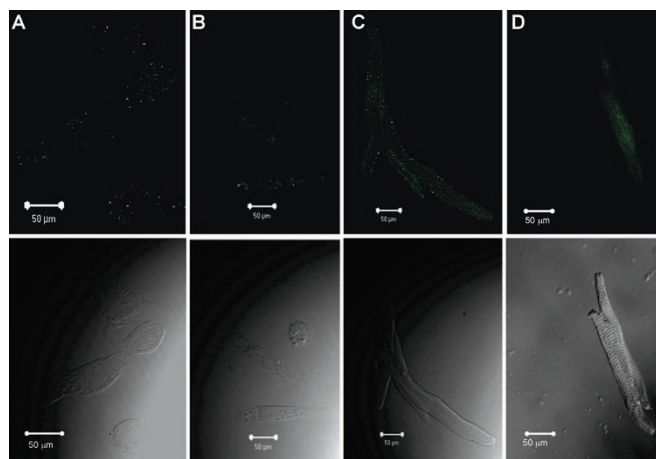


**Figure 4.** Representative confocal images of negative controls using anti- $\alpha_{1D}$   $Ca^{2+}$  channel antibody preincubated with its antigenic peptide: *A*, fetal atrial cells; *B*, neonatal atrial cells; *C*, 6-wk atrial cells; *D*, 6-mo atrial cell. *Arrows* indicate the nucleus.

incubated with its antigenic peptide (Fig. 4A and B) and with the secondary antibody alone (data not shown). Immunostaining intensity across the cells was assessed by surface plot and shows that the  $\alpha_{1D}$  protein is present at the sarcolemma but is more prominent at the nuclear region of fetal and neonatal stages (Fig. 5A and B), compared with adult stages (Fig. 5C and D).

**Expression of the  $\alpha_{1D}$   $Ca^{2+}$  channel in adult atrial HL-1 cells.** To confirm that the nuclear staining was unique only to the immature cells, we took advantage of a tumor-derived

mouse atrial cell line, HL-1 cells, to perform immunostaining using the anti- $\alpha_{1D}$  antibody. The unique feature of the HL-1 cells is that they retain the properties of the normal adult atrial cells, but ultrastructurally resemble immature mitotic mouse atrial myocytes. The expression of  $\alpha_{1D}$   $Ca^{2+}$  channel in HL-1 cells was demonstrated by RT-PCR using the  $\alpha_{1D}$  specific primer (Fig. 6A) and by Western blot (Fig. 6B) using the anti- $\alpha_{1D}$  antibody. Interestingly, in these HL-1 cells, the  $\alpha_{1D}$   $Ca^{2+}$  channel was found to be on the sarcolemma and also in the nucleus, a staining pattern that is indistinguishable from that of the fetal and neonatal cardiac myocytes (Fig. 6C), suggesting that the  $\alpha_{1D}$   $Ca^{2+}$  channel might play unique roles in the immature cardiac cells.

## DISCUSSION

Although the developmental expression profile of the  $\alpha_{1C}$   $Ca^{2+}$  channel has been extensively studied previously (11,13,19), to date, no such information is available for the  $\alpha_{1D}$   $Ca^{2+}$  channel. This study is the first to characterize the expression and subcellular localization of  $\alpha_{1D}$   $Ca^{2+}$  channel during heart development. The striking findings of this study are the abundant level, the universal expression, the unique nuclear localization, and the existence of the full-length (250 kD)  $\alpha_{1D}$   $Ca^{2+}$  channel in the immature heart. In contrast, only the short form (190 kD) of the  $\alpha_{1D}$   $Ca^{2+}$  channel was expressed in the adult stage and its expression is restricted to the atria but not to the ventricles. Interestingly, the nuclear localization of the  $\alpha_{1D}$   $Ca^{2+}$  channel was not observed in the adult atrial cells.



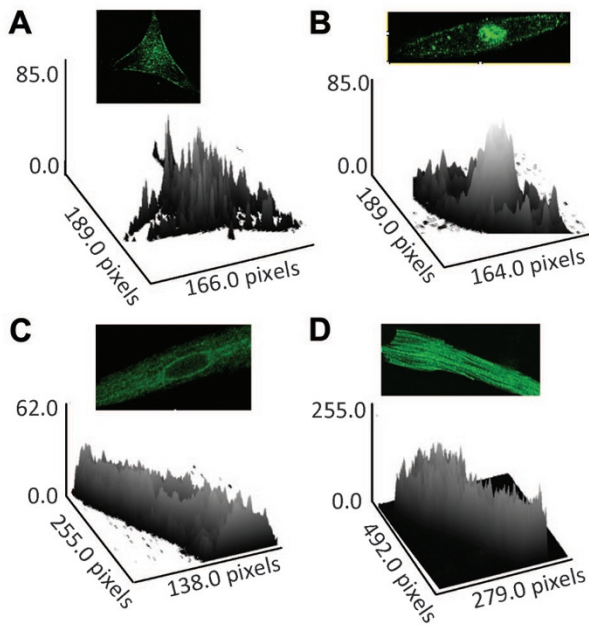


**Figure 5.** Surface plots corresponding to Figure 2 showing staining intensity of the  $\alpha_{1D}$  protein across the atrial cells including sarcolemma and perinuclear regions at different developmental stages. A, fetal; B, neonatal; C, 6-weeks; D, 6-months. Note prominent nuclear staining at both fetal and neonatal stages compared with adult stages.

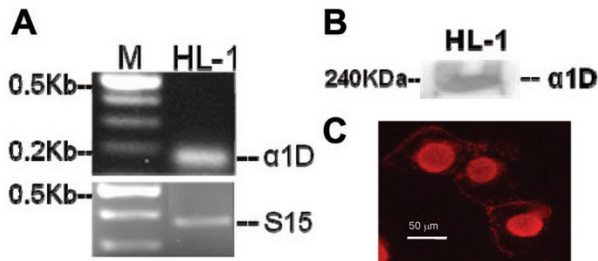


**Figure 6.** (A) Expression and localization of  $\alpha_{1D}$  Ca channel in HL-cells: Transcript of 180 bp corresponding to the  $\alpha_{1D}$  Ca<sup>2+</sup> channel was amplified from HL-1 cells. A 361-bp housekeeping gene S15 confirms accuracy of cDNA integrity and gel loading techniques. M indicates markers. (B) Expression of the  $\alpha_{1D}$  Ca<sup>2+</sup> channel protein in HL-1 cells by Western blot using anti- $\alpha_{1D}$  Ca<sup>2+</sup> channel antibody. (C) Confocal immunostaining of the  $\alpha_{1D}$  Ca<sup>2+</sup> channels in HL-1 cells using anti- $\alpha_{1D}$  Ca<sup>2+</sup> channel antibody.

Altogether, the data suggest that the  $\alpha_{1D}$  Ca<sup>2+</sup> channel may play unique roles in the immature heart. However, because of the unavailable pharmacological or biophysical approaches to separate the  $\alpha_{1D}$  from the  $\alpha_{1C}$  channel currents, the functional relevance of the  $\alpha_{1D}$  Ca<sup>2+</sup> channel during heart development was not sought.

**Distinct subcellular localization of the  $\alpha_{1D}$  Ca<sup>2+</sup> channel at different developmental stages.** An intriguing observation of this study is the age-dependent subcellular localization of the  $\alpha_{1D}$  Ca<sup>2+</sup> channel. While in the fetal and neonatal stages, the  $\alpha_{1D}$  Ca<sup>2+</sup> channel is highly expressed in the nucleus in addition to the sarcolemma, it gradually moves to the perinuclear region and eventually resolves from the perinuclear areas at the adult stage. The specificity of the nuclear/perinuclear staining was confirmed with different experimental ap-

proaches. First, the anti- $\alpha_{1D}$  Ca<sup>2+</sup> channel antibodies from two commercial resources yielded the same staining patterns. Second, the nuclear staining was not observed when the anti- $\alpha_{1D}$  antibody was preincubated with its antigenic peptide. Third, using the same antibody, the nuclear staining was observed in only the fetal and the neonatal stages but not in the adult stage. Fourth, the  $\alpha_{1D}$  Ca<sup>2+</sup> channel was observed in the nucleus of adult atrial HL-1 cells, which possess properties of the immature cardiac cells. Finally, consistent with the present results, Zhang *et al.* (7), using the same anti- $\alpha_{1D}$  antibody (Calbiochem, San Diego, CA), showed similar staining pattern for the adult atrial cells, in which the nuclear staining was not observed. Furthermore, this anti- $\alpha_{1D}$  antibody did not show any specific staining in atrial cells from the  $\alpha_{1D}$  Ca<sup>2+</sup> channel knockout mice. We have also ruled out the possibility that the observed nuclear staining may be an artifact associated with the cultures of fetal and neonatal atrial and ventricular cells because similar staining patterns of the  $\alpha_{1D}$  Ca<sup>2+</sup> channel were also observed in freshly isolated human fetal cardiac cells (15). Altogether, these data demonstrate that the nuclear staining in fetal and neonatal cardiac myocytes is specific. Further support for this nuclear/perinuclear localization of the  $\alpha_{1D}$  Ca<sup>2+</sup> channel is that the expression of ion channels in the nucleus has been reported for Cl channels, Ca-ATPases, InsP<sub>3</sub> receptors, and K channels (20–24). The exact role of the  $\alpha_{1D}$  Ca<sup>2+</sup> channel in the nucleus is not yet known and warrant further investigations.

It is also noteworthy that the  $\alpha_{1D}$  Ca<sup>2+</sup> channel was not expressed in the adult rat ventricles. This observation is supported by studies from Takemura *et al.* (25), who showed similar result, and by Zhang *et al.* (7), who showed a significantly lesser expression levels of the  $\alpha_{1D}$  Ca<sup>2+</sup> channel in the adult mice ventricles. This developmental expression pattern for the  $\alpha_{1D}$  Ca<sup>2+</sup> channel is strikingly similar to that of the T-type Ca<sup>2+</sup> channel (11) with the exception that the T-type Ca<sup>2+</sup> channel is reexpressed in the adult ventricles under pathological conditions (26,27). Whether the  $\alpha_{1D}$  Ca<sup>2+</sup> channel is reexpressed in the adult ventricles under pathological conditions remains to be determined.

**Expression levels of the  $\alpha_{1D}$  Ca<sup>2+</sup> channel in the heart at different stages.** Studies involving with developmental changes have faced the challenge of choosing an internal control with invariant expression. Among the commonly used internal control housekeeping genes, such as glyceraldehydes phosphate dehydrogenase (GAPDH),  $\beta$ -actin, and ribosomal RNA (18S and 28S), 18S rRNA seems to be the better standard as it shows constant levels throughout gestation and its expression does not appear to vary between individuals (28,29). On the other hand, the expression level of GAPDH and  $\beta$ -actin varies across tissues during cell proliferation (28,30). Significant variation in GAPDH expression has also been reported between individuals and during development (28,29,31). In this study,  $\alpha_{1D}$  Ca<sup>2+</sup> channel mRNA level, determined by real-time RT-PCR using 18S rRNA as an internal control, decreased after birth. Postnatal decrease of the  $\alpha_{1D}$  Ca<sup>2+</sup> channel mRNA was paralleled by the protein level determined

by Western blot. Physiologically, the more abundant expression of the  $\alpha_{1D}$   $Ca^{2+}$  channel in the fetal cardiac stage is likely beneficial because of the low levels of the  $\alpha_{1C}$   $Ca^{2+}$  channel expression (19,32) and for the less abundant sarcoplasmic reticulum in the fetal heart compared with the adult heart (33,34).

Despite the abundant expression of the  $\alpha_{1D}$   $Ca^{2+}$  channel in the fetal stage, the knockout of the  $\alpha_{1C}$   $Ca^{2+}$  channel in mice is embryonic lethal at d 14.5 postcoitum (35), while the  $\alpha_{1D}^{-/-}$  mice survives (5,7,36). This suggests that the  $\alpha_{1D}$   $Ca^{2+}$  channel in the immature heart may be important to cellular functions other than excitation-coupling. Indeed, the unique nuclear localization of the  $\alpha_{1D}$  channel in the fetal and neonatal stages also points to other unique functions of the  $\alpha_{1D}$  in the immature hearts.

**Two forms of the  $\alpha_{1D}$   $Ca^{2+}$  channel are present in the immature hearts.** Two forms of the  $\alpha_{1D}$   $Ca^{2+}$  channel protein, a full length (250 kD) and a short form (190 kD) were observed in the immature heart. A splicing site at the C-terminal region of  $\alpha_{1D}$  has been reported (37,38). A 58-bp deletion results in a frame shift that produces a premature termination codon giving rise to the  $\alpha_{1D}$  subunit that differs in length by 535 amino acid, with a corresponding molecular weight of 190 kD (37,38). On the other hand, experiments in the cardiac myocytes and neurons indicate that the C terminus of the  $\alpha_{1C}$  channel is proteolytically cleaved, yielding a truncated channel (39,40), with the full length observed in only the fetal heart (13,41), indicating an increased proteolytic activity in the adult heart. The authors also reported a novel mechanism of the  $\alpha_{1C}$  channel-associated transcription regulation in which the proteolytic C-terminal fragment of the  $\alpha_{1C}$   $Ca^{2+}$  channel translocates to the nucleus and regulates gene transcriptions (41). It is unclear whether these two sizes of  $\alpha_{1D}$  protein observed in this study are the products of proteolytic activity or splicing variant. Whether these spliced variants are developmentally regulated and whether the observed differential localization of the protein is related to the expression of different splice variants are unknown and warrant further investigations.

In conclusion, the  $\alpha_{1D}$   $Ca^{2+}$  channel is a newly discovered L-type  $Ca^{2+}$  channel isoform in the heart. It has distinct age-dependent expression and subcellular localization, suggesting unique function during heart development.

**Acknowledgments.** We thank Dr. Seino and Dr. Striessnig for providing the plasmids used in this study.

## REFERENCES

- Catterall WA, Perez-Reyes E, Snutch TP, Striessnig J 2005 International Union of Pharmacology. XLVIII. Nomenclature and structure-function relationships of voltage-gated calcium channels. *Pharmacol Rev* 57:411–425
- Ertel EA, Campbell KP, Harpold MM, Hofmann F, Mori Y, Perez-Reyes E, Schwartz A, Snutch TP, Tanabe T, Birnbaumer L, Tsien RW, Catterall WA 2000 Nomenclature of voltage-gated calcium channels. *Neuron* 25:533–535
- Hell JW, Westenbroek RE, Warner C, Ahljianian MK, Prystay W, Gilbert MM, Snutch TP, Catterall WA 1993 Identification and differential subcellular localization of the neuronal class C and class D L-type calcium channel  $\alpha_1$  subunits. *J Cell Biol* 123:949–962
- Seino S, Chen L, Seino M, Blondel O, Takeda J, Johnson JH, Bell GI 1992 Cloning of the  $\alpha_1$  subunit of a voltage-dependent calcium channel expressed in pancreatic beta cells. *Proc Natl Acad Sci USA* 89:584–588
- Mangoni ME, Couette B, Bourinet E, Platzer J, Reimer D, Striessnig J, Nargeot J 2003 Functional role of L-type Cav1.3  $Ca^{2+}$  channels in cardiac pacemaker activity. *Proc Natl Acad Sci USA* 100:5543–5548
- Matthes J, Yildirim L, Wietzorrek G, Reimer D, Striessnig J, Herzig S 2004 Disturbed atrio-ventricular conduction and normal contractile function in isolated hearts from Cav1.3-knockout mice. *Naunyn Schmiedebergs Arch Pharmacol* 369:554–562
- Zhang Z, He Y, Tuteja D, Xu D, Timofeyev V, Zhang Q, Glatzer KA, Xu Y, Shin HS, Low R, Chiamvimonvat N 2005 Functional roles of Cav1.3( $\alpha_1D$ ) calcium channels in atria: insights gained from gene-targeted null mutant mice. *Circulation* 112:1936–1944
- Mancarella S, Yue Y, Karnabi E, Qu Y, El Sherif N, Boutjdir M 2008 Impaired calcium homeostasis is associated with atrial fibrillation in the  $\alpha_1D$  L-type  $Ca^{2+}$  channel KO mouse. *Am J Physiol Heart Circ Physiol* 2008:H2017–H2024
- Bell DC, Butcher AJ, Berrow NS, Page KM, Brust PF, Nesterova A, Stauderman KA, Seabrook GR, Nurnberg B, Dolphin AC 2001 Biophysical properties, pharmacology, and modulation of human, neuronal L-type ( $\alpha_1D$ ),  $Ca(V)1.3$  voltage-dependent calcium currents. *J Neurophysiol* 85:816–827
- Koschak A, Reimer D, Huber I, Grabner M, Glossmann H, Engel J, Striessnig J 2001  $\alpha_1D$  (Cav1.3) subunits can form L-type  $Ca^{2+}$  channels activating at negative voltages. *J Biol Chem* 276:22100–22106
- Qu Y, Boutjdir M 2001 Gene expression of SERCA2a and L- and T-type Ca channels during human heart development. *Pediatr Res* 50:569–574
- Brillantes AM, Bezprozvannaya S, Marks AR 1994 Developmental and tissue-specific regulation of rabbit skeletal and cardiac muscle calcium channels involved in excitation-contraction coupling. *Circ Res* 75:503–510
- Liu L, O'Hara DS, Cala SE, Poornima I, Hines RN, Marsh JD 2000 Developmental regulation of the L-type calcium channel  $\alpha_1C$  subunit expression in heart. *Mol Cell Biochem* 205:101–109
- Qu Y, Karnabi E, Chahine M, Vassalle M, Boutjdir M 2007 Expression of skeletal muscle Na(V)1.4 Na channel isoform in canine cardiac Purkinje myocytes. *Biochem Biophys Res Commun* 355:28–33
- Qu Y, Baroudi G, Yue Y, Boutjdir M 2005 Novel molecular mechanism involving  $\alpha_1D$  (Cav1.3) L-type calcium channel in autoimmune-associated sinus bradycardia. *Circulation* 111:3034–3041
- Boutjdir M, Chen L, Zhang ZH, Tseng CE, El-Sherif N, Buyon JP 1998 Serum and immunoglobulin G from the mother of a child with congenital heart block induce conduction abnormalities and inhibit L-type calcium channels in a rat heart model. *Pediatr Res* 44:11–19
- Ogawa E, Saito Y, Harada M, Kamitani S, Kuwahara K, Miyamoto Y, Ishikawa M, Hamanaka I, Kajiyama N, Takahashi N, Nakagawa O, Masuda I, Kishimoto I, Nakao K 2000 Outside-in signalling of fibronectin stimulates cardiomyocyte hypertrophy in cultured neonatal rat ventricular myocytes. *J Mol Cell Cardiol* 32:765–776
- Qu Y, Baroudi G, Yue Y, El-Sherif N, Boutjdir M 2005 Localization and modulation of  $\alpha_1D$  (Cav1.3) L-type Ca channel by protein kinase A. *Am J Physiol Heart Circ Physiol* 288:H2123–H2130
- Huynh TV, Chen F, Wetzel GT, Friedman WF, Klitzner TS 1992 Developmental changes in membrane  $Ca^{2+}$  and  $K^+$  currents in fetal, neonatal, and adult rabbit ventricular myocytes. *Circ Res* 70:508–515
- Draguhn A, Borner G, Beckmann R, Buchner K, Heinemann U, Hucho F 1997 Large-conductance cation channels in the envelope of nuclei from rat cerebral cortex. *J Membr Biol* 158:159–166
- Franco-Obrégón A, Wang HW, Clapham DE 2000 Distinct ion channel classes are expressed on the outer nuclear envelope of T- and B-lymphocyte cell lines. *Biophys J* 79:202–214
- Stehno-Bittel L, Perez-Terzic C, Luckhoff A, Clapham DE 1996 Nuclear ion channels and regulation of the nuclear pore. *Soc Gen Physiol Ser* 51:195–207
- Stehno-Bittel L, Luckhoff A, Clapham DE 1995 Calcium release from the nucleus by InsP3 receptor channels. *Neuron* 14:163–167
- Maruyama Y, Shimada H, Taniguchi J 1995  $Ca^{2+}$ -activated  $K^{+}$ -channels in the nuclear envelope isolated from single pancreatic acinar cells. *Pflugers Arch* 430:148–150
- Takemura H, Yasui K, Opthof T, Niwa N, Horiba M, Shimizu A, Lee JK, Honjo H, Kamiya K, Ueda Y, Kodama I 2005 Subtype switching of L-Type  $Ca^{2+}$  channel from Cav1.3 to Cav1.2 in embryonic murine ventricle. *Circ J* 69:1405–1411
- Nuss HB, Houser SR 1993 T-type  $Ca^{2+}$  current is expressed in hypertrophied adult feline left ventricular myocytes. *Circ Res* 73:777–782
- Martínez ML, Heredia MP, Delgado C 1999 Expression of T-type  $Ca^{2+}$  channels in ventricular cells from hypertrophied rat hearts. *J Mol Cell Cardiol* 31:1617–1625
- Bas A, Forsberg G, Hammarstrom S, Hammarstrom ML 2004 Utility of the housekeeping genes 18S rRNA, beta-actin and glyceraldehyde-3-phosphate-dehydrogenase for normalization in real-time quantitative reverse transcriptase-polymerase chain reaction analysis of gene expression in human T lymphocytes. *Scand J Immunol* 59:566–573
- Patel P, Boyd CA, Johnston DG, Williamson C 2002 Analysis of GAPDH as a standard for gene expression quantification in human placenta. *Placenta* 23:697–698
- Mansur NR, Meyer-Siegler K, Wurzer JC, Sirover MA 1993 Cell cycle regulation of the glyceraldehyde-3-phosphate dehydrogenase/uracil DNA glycosylase gene in normal human cells. *Nucleic Acids Res* 21:993–998
- Oikarinen A, Makela J, Vuorio T, Vuorio E 1991 Comparison on collagen gene expression in the developing chick embryo tendon and heart. Tissue and development time-dependent action of dexamethasone. *Biochim Biophys Acta* 1089:40–46
- Boucek RJ Jr, Shelton M, Artman M, Mushlin PS, Starnes VA, Olson RD 1984 Comparative effects of verapamil, nifedipine, and diltiazem on contractile function in the isolated immature and adult rabbit heart. *Pediatr Res* 18:948–952

33. Hoerter J, Mazet F, Vassort G 1981 Perinatal growth of the rabbit cardiac cell: possible implications for the mechanism of relaxation. *J Mol Cell Cardiol* 13:725–740
34. Maylie JG 1982 Excitation-contraction coupling in neonatal and adult myocardium of cat. *Am J Physiol* 242:H834–H843
35. Xu M, Welling A, Paparisto S, Hofmann F, Klugbauer N 2003 Enhanced expression of L-type Cav1.3 calcium channels in murine embryonic hearts from Cav1.2-deficient mice. *J Biol Chem* 278:40837–40841
36. Zhang Z, Xu Y, Song H, Rodriguez J, Tuteja D, Namkung Y, Shin HS, Chiamvimonvat N 2002 Functional Roles of Ca(v)1.3 (alpha1D) calcium channel in sinoatrial nodes: insight gained using gene-targeted null mutant mice. *Circ Res* 90:981–987
37. Safa P, Boulter J, Hales TG 2001 Functional properties of Cav1.3 (alpha1D) L-type Ca<sup>2+</sup> channel splice variants expressed by rat brain and neuroendocrine GH3 cells. *J Biol Chem* 276:38727–38737
38. Scholze A, Plant TD, Dolphin AC, Nurnberg B 2001 Functional expression and characterization of a voltage-gated CaV1.3 (alpha1D) calcium channel subunit from an insulin-secreting cell line. *Mol Endocrinol* 15:1211–1221
39. De Jongh KS, Colvin AA, Wang KK, Catterall WA 1994 Differential proteolysis of the full-length form of the L-type calcium channel alpha 1 subunit by calpain. *J Neurochem* 63:1558–1564
40. Gerhardstein BL, Gao T, Bunemann M, Puri TS, Adair A, Ma H, Hosey MM 2000 Proteolytic processing of the C terminus of the alpha(1C) subunit of L-type calcium channels and the role of a proline-rich domain in membrane tethering of proteolytic fragments. *J Biol Chem* 275:8556–8563
41. Gomez-Ospina N, Tsuruta F, Barreto-Chang O, Hu L, Dolmetsch R 2006 The C terminus of the L-type voltage-gated calcium channel Ca(V)1.2 encodes a transcription factor. *Cell* 127:591–606